

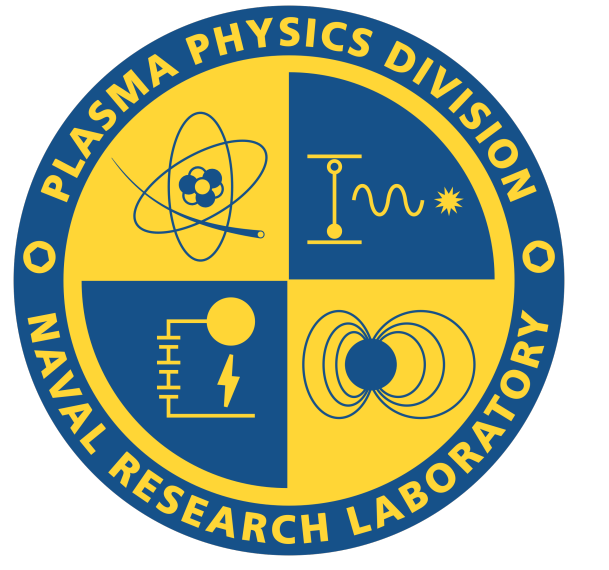
# Magnetohydrodynamic Approximations of the m=0 Rayleigh-Taylor Instability in a Z-Pinch



Andrew Jiao<sup>1</sup>, A. S. Richardson<sup>2</sup>

<sup>1</sup>Contractor to NRL through the ONR NREIP program

<sup>2</sup>Naval Research Laboratory, Plasma Physics Division



This work was supported by the Office of Naval Research NREIP program and the Naval Research Laboratory Base Program.

**Abstract** The m=0 instability of the pinching plasma column in the Z-pinch and dense plasma focus (DPF) is thought to be important in generating a high energy ion beam which can drive neutron-producing beam target D-D fusion reactions. Since ion beams cannot be generated in ideal magnetohydrodynamic (MHD) models of the Z-pinch and DPF, various non-ideal fluid models are being examined for creating high energy ion beams. Linear growth rates of the m=0 Rayleigh-Taylor (RT) instability in the ideal and extended MHD models are compared. The roles of the resistive, Hall, and electron pressure terms in the generalized Ohm's law are examined. Implications of these non-ideal effects as mechanisms of ion acceleration are discussed.

**Introduction** NRL has recently begun a program to investigate charged particle acceleration in imploding plasmas using a DPF driven by the Hawk pulsed-power generator. [1] As part of the program, theoretical approaches combining kinetic PIC and fluid models are being explored, the latter being well-suited to capture plasma compression dynamics and the growth of the RT instability. We use the MHD model and diagnose the effects of the non-ideal terms on the m=0 "sausage" instability, well-known to be one of the most dangerous instabilities in imploding plasmas. [2, 3]

Coupled to Maxwell's equations, the MHD equations are given as

$$\begin{aligned} \frac{\partial \rho}{\partial t} + \nabla \cdot (\rho \mathbf{V}) &= 0 \\ \rho \frac{\partial \mathbf{V}}{\partial t} + \rho(\mathbf{V} \cdot \nabla) \mathbf{V} &= -\nabla P + \frac{1}{c} \mathbf{J} \times \mathbf{B} \\ \frac{\partial P}{\partial t} + (\mathbf{V} \cdot \nabla) P + \gamma P \nabla \cdot \mathbf{V} &= (\gamma - 1) \eta J^2 \\ (1) \quad \frac{m_e m_i}{\rho e^2} \frac{\partial \mathbf{J}}{\partial t} &= \frac{m_i}{2\rho e} \nabla P + \mathbf{E} + \frac{1}{c} \mathbf{V} \times \mathbf{B} - \frac{m_i}{\rho e c} \mathbf{J} \times \mathbf{B} - \eta \mathbf{J} \end{aligned}$$

We use the equation of state for an ideal hydrogen gas  $\rho = m_i P / 2T$ . We are interested in low-frequency physics that allow us to neglect the displacement current and the electron inertia. We take the ratio of specific heats to be  $\gamma=2$ .

**Bennett Equilibrium** Our test case is a steady-state configuration that balances the plasma and magnetic pressures in a plasma filament:  $\partial_t \mathbf{V} = \mathbf{V} = 0$ . Given a pressure profile

$$P(r) = P_0 \left( 0.05 + e^{-(r/r_0)^n} \right), \quad P_0 = \frac{B_0^2}{4\pi}, \quad B_0 = \frac{2I}{r_0 c}$$

for integer n, the momentum equation and its solution (in normalized units) given appropriate boundary conditions are

$$\frac{\partial}{\partial r} \left( P + \frac{B^2}{8\pi} \right) + \frac{2}{r} \frac{B^2}{8\pi} = 0, \quad \frac{B^2}{8\pi} = \frac{2}{nr^2} \int_0^{r^2} \xi^{2/n-1} e^{-\xi} d\xi - e^{-r^n}$$

where the integral is the lower incomplete gamma function. The initial density is found by setting the initial temperature T=1 to be uniform in r.

The balance of the plasma and magnetic pressures in cylindrical coordinates also introduces a coordinate source term resulting from the magnetic tension (curvature of the field lines). This term plays the role of the local gravitational acceleration which is then evaluated at the radius of the plasma filament

$$(2) \quad g = \frac{B^2}{4\pi \rho r_0}$$

**Linear Stability Analysis** We examine the stability of the azimuthally symmetric m=0 mode by linearizing the MHD equations about the equilibrium we found. The induction equation is obtained using Faraday's law and the generalized Ohm's law (1). In the ideal MHD case, this equation is

$$\frac{\partial \mathbf{B}}{\partial t} = \nabla \times (\mathbf{V} \times \mathbf{B})$$

The MHD equations are Fourier transformed like  $(t, z) \rightarrow (\omega, k)$  and the resulting r-dependent equations are solved as an eigenvalue problem in  $\omega$  and the state vector  $(\rho_1, P_1, V_1, B_1)^T$ . The equations are discretized using central-difference methods and formed into a block matrix. The resulting eigenfunctions are normalized and assigned an amplitude of 0.05. We used Ampere's law and (1) to find  $\mathbf{J}$ ,  $\mathbf{E}$ , and vorticity  $\Omega = \nabla \times \mathbf{V}$ . T was found using the equation of state.

To first order,  $B_{r1}$ ,  $B_{z1}$ , and  $V_{\theta1}$  all vanish. This remains true when including non-ideal effects. The eigenvalue equations are subject to the boundary conditions

$$\begin{aligned} \frac{\partial \rho_1}{\partial r} = \frac{\partial P_1}{\partial r} = B_{\theta1} = V_{r1} = \frac{\partial V_{z1}}{\partial r} &= 0 \quad \text{at } r = 0 \\ \rho_1 = P_1 = B_{\theta1} = \frac{\partial V_{r1}}{\partial r} = V_{z1} &= 0 \quad \text{at } r = r_{\max} \end{aligned}$$

The condition  $\partial_r V_{r1}(r_{\max}) = 0$  is important to maintain the numerical stability of the solution.

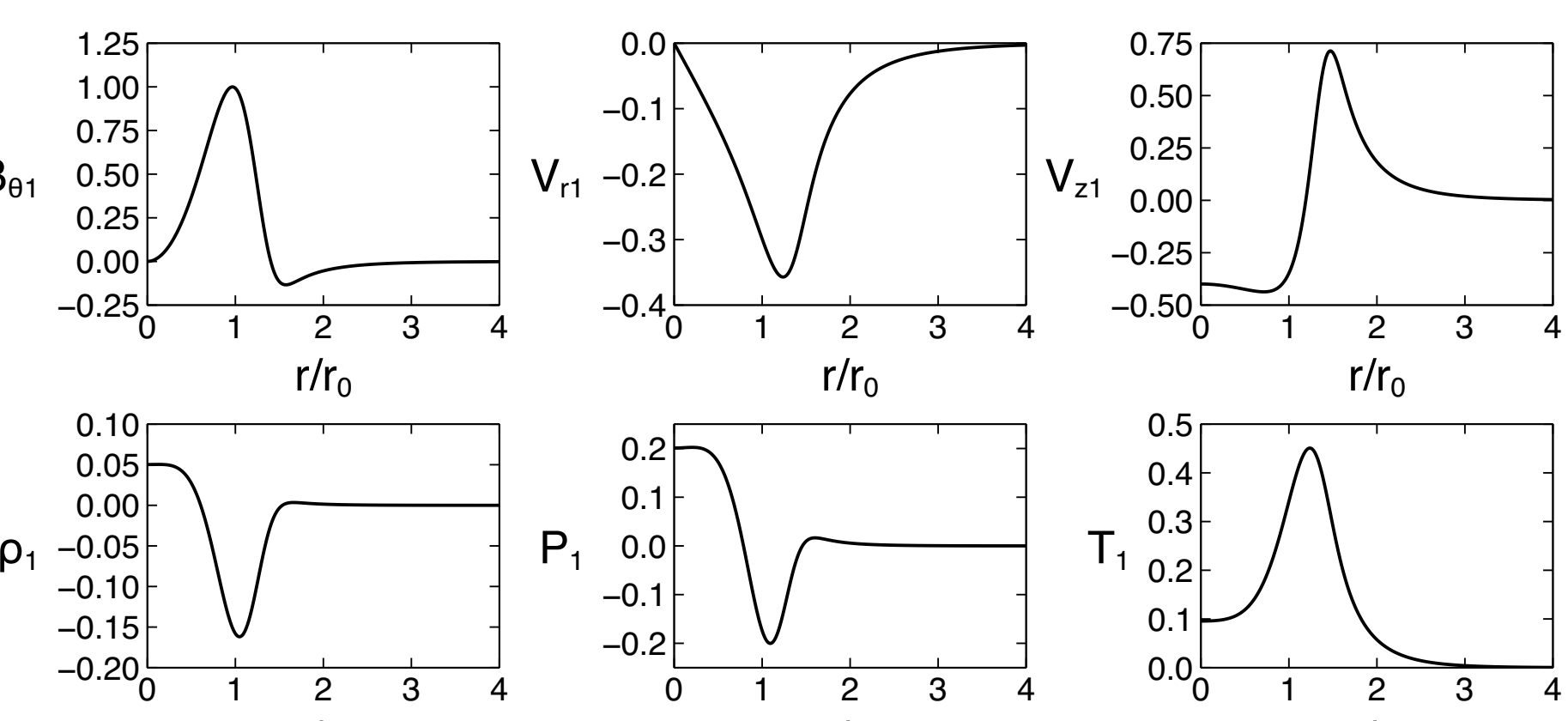


Figure 1. Normalized perturbations of variables in ideal MHD at the lineouts  $z=0$ . Note that  $V_{z1}$  is  $r/2$  out of phase with  $V_{r1}$ .

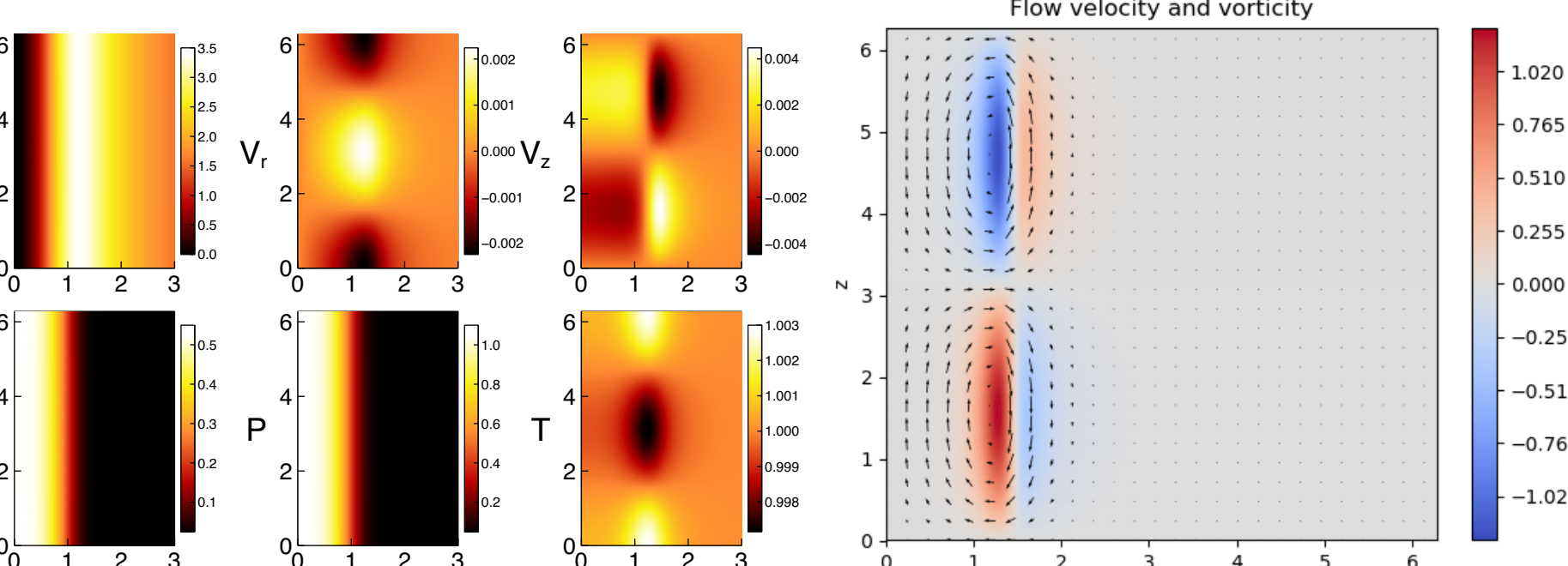


Figure 2. Contours of variables in the ideal MHD system, showing the  $r/r_2$  phase shift in  $V_z$ .

Figure 3.  $\mathbf{V}$  and  $\Omega_\theta$  in the r-z plane. Note that the positive  $\theta$  direction points into the board.

**Non-Ideal Terms** The addition of non-ideal terms in (1) results in the induction equation being modified to

$$\frac{\partial \mathbf{B}}{\partial t} = \nabla \times (\mathbf{V} \times \mathbf{B}) + \frac{c^2 \eta}{4\pi} \nabla^2 \mathbf{B} - \frac{m_i c}{4\pi e} \nabla \times \left[ \frac{1}{\rho} (\nabla \times \mathbf{B}) \times \mathbf{B} \right] - \frac{m_i c}{2e} \frac{\nabla p \times \nabla P}{\rho^2}$$

where on the right hand side, we have respective contributions from the ideal, resistive, Hall, and electron pressure terms. Their coefficients are conveniently denoted by  $D_\eta$ ,  $D_H$ , and  $D_P$ . Since the Joule heating term is quadratic in  $\mathbf{J}$ , it does not contribute to the energy equation in the linear analysis. We also assume that the diffusivity is uniform in the plasma.

Non-zero Hall and electron pressure terms gives complex eigenvalues and eigenfunctions even after correcting for an overall phase, suggesting that these modes are both growing and oscillating. Due to the initial  $J_z$ , the resistive  $\mathbf{E}$  field will point mostly in the z direction. Since the coefficients in the Hall and electron pressure terms are related by a factor of  $2\pi$ , we find that the electron pressure contribution to  $E_r$  halves the  $E_r$  generated by the Hall field. However, the presence of these terms still distorts the contours of the electric field.

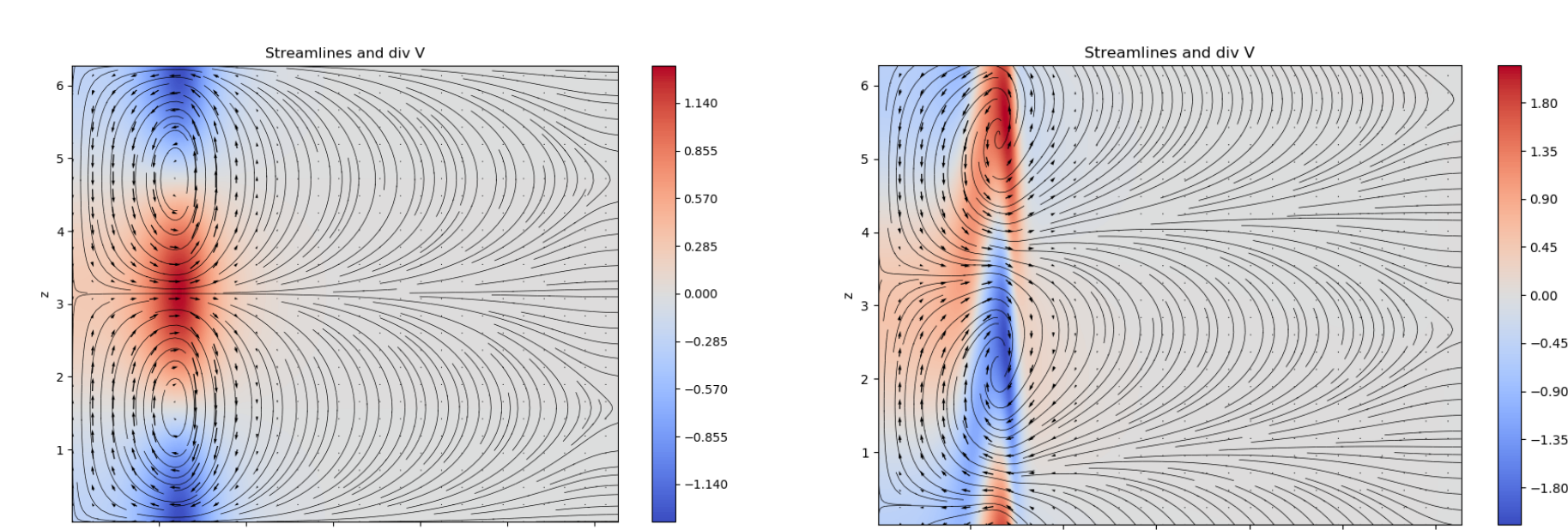


Figure 4. Streamlines of  $\mathbf{V}$  and  $\text{div } \mathbf{V}$  for the ideal (left) and Hall (right) MHD system with  $D_H=0.1$ .

**Growth Rates** A classic result from hydrodynamic stability concerns the growth rate of the Rayleigh-Taylor instability in a slab geometry where a denser fluid sits on top of a lighter fluid. The result is known to be  $\gamma^2 = gk$ , [4] which holds for the ideal MHD in a cylindrical geometry in the  $k \ll 1$  limit when g is given by (2). In the limit that  $k \gg 1$ , the growth rate asymptotes to  $\gamma^2 \sim g/r_1$ , where  $r_1$  is the characteristic length scale of the gradient. [5] Convergence tests were done to check that  $\gamma$  was converging with increasing resolution at a fixed  $k$ .

Numerical calculations were done in both Cartesian and cylindrical coordinates with the same initial pressure profile, the former adding gravity to the momentum equation. We found that calculations in both coordinates agree with the results in [5].

The presence of the resistive term corresponds to magnetic diffusion and contributes to a  $-k^2$  after Fourier transforming, which damps higher modes and allows us to observe a peak in the  $\gamma(k)$  relation.

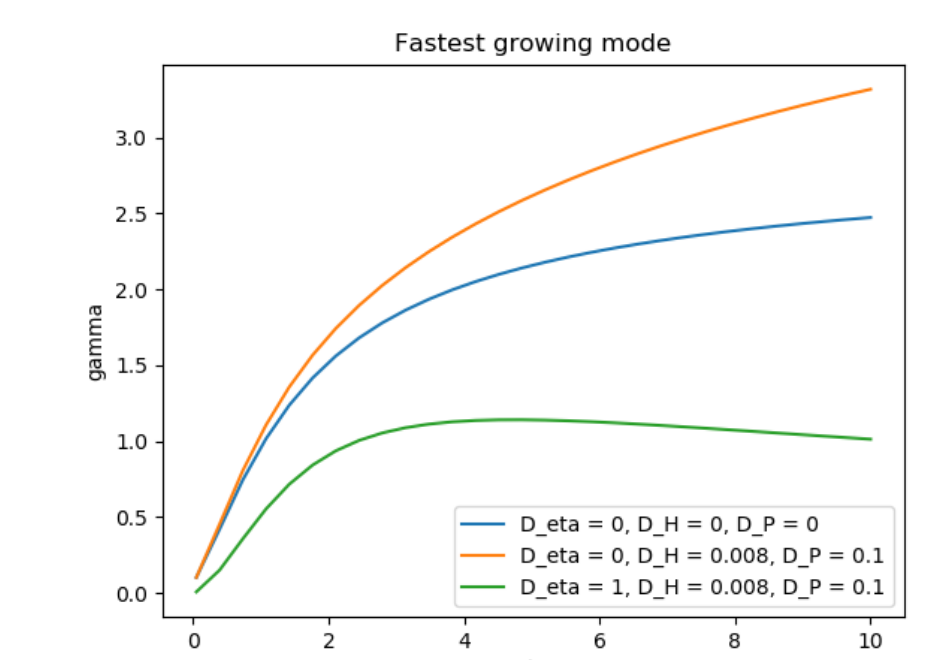


Figure 5. Growth rates with ideal/non-ideal terms.

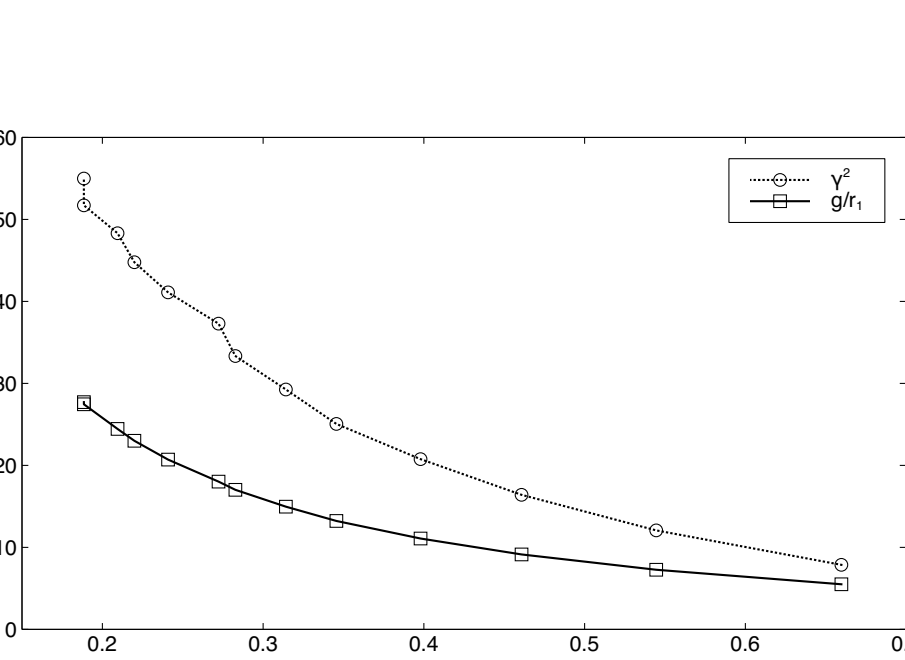


Figure 6.  $\gamma^2$  and  $g/r_1$  with 600 grid points.

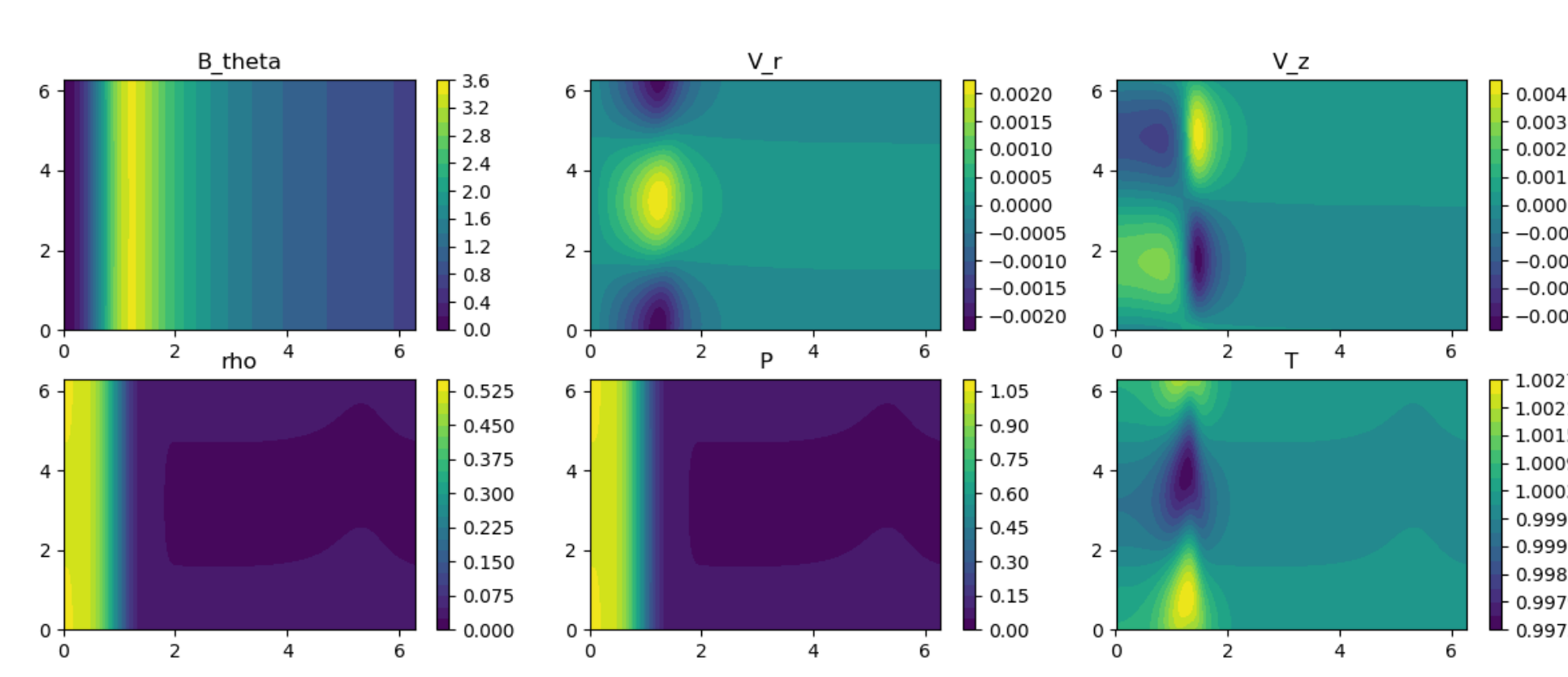


Figure 7. Contours of variables in the Hall MHD system for  $D_H=0.01$ .

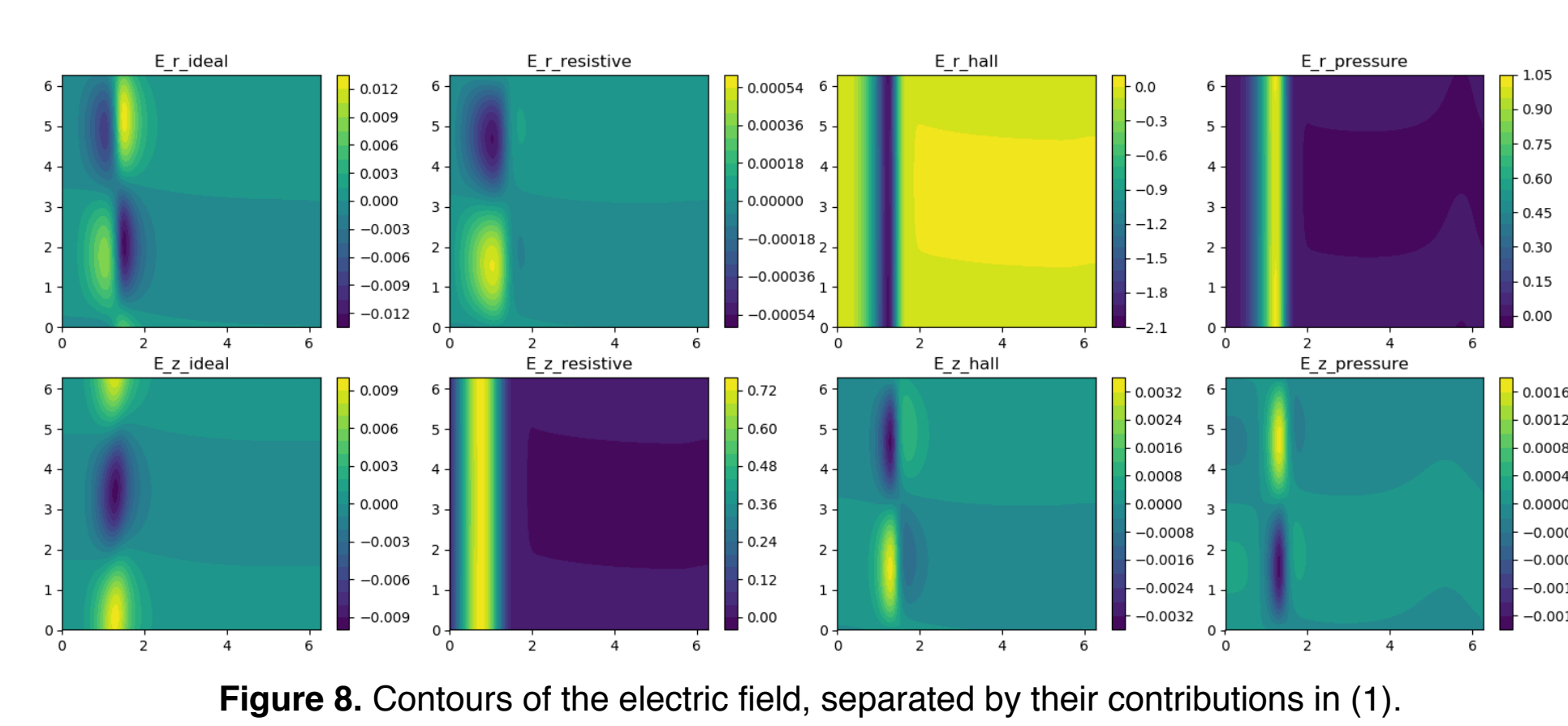


Figure 8. Contours of the electric field, separated by their contributions in (1). Coefficients are  $D_\eta=0.1$ ,  $D_P=0.1$ , and  $D_H=D_P/2\pi$ .

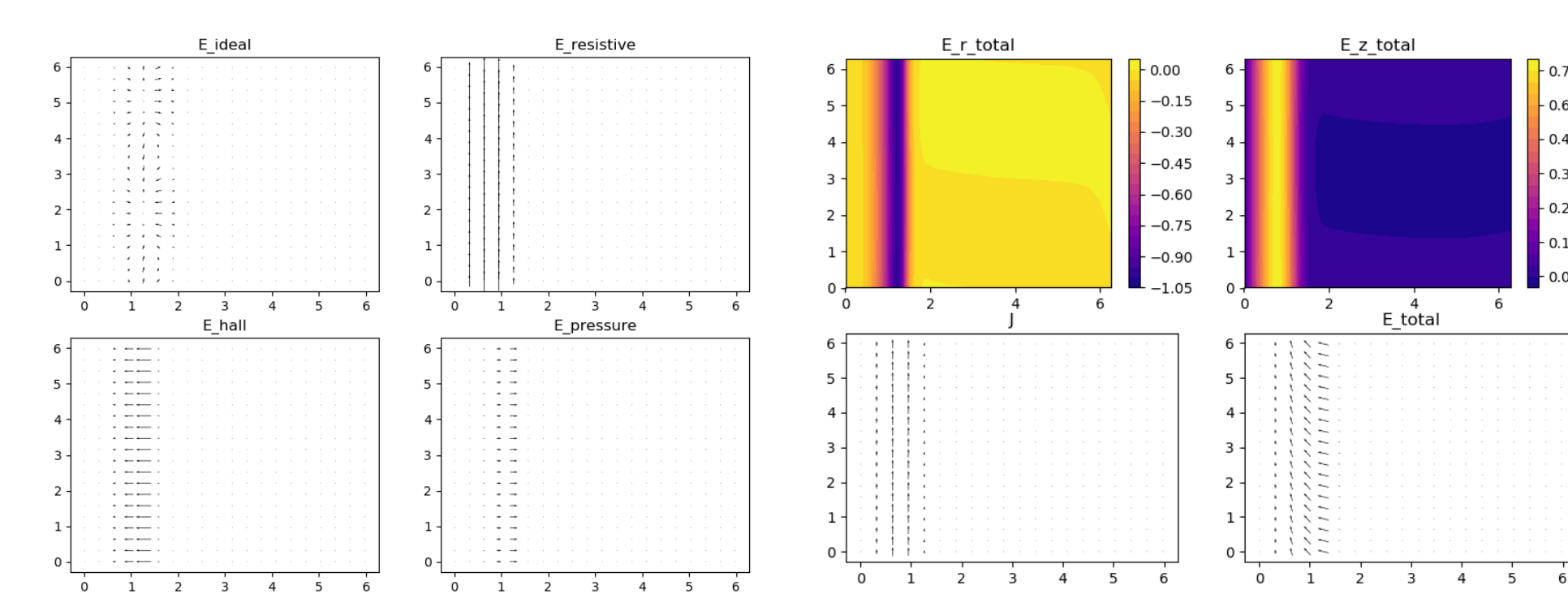


Figure 9. Quiver plots of  $\mathbf{E}$ , separated by (1).

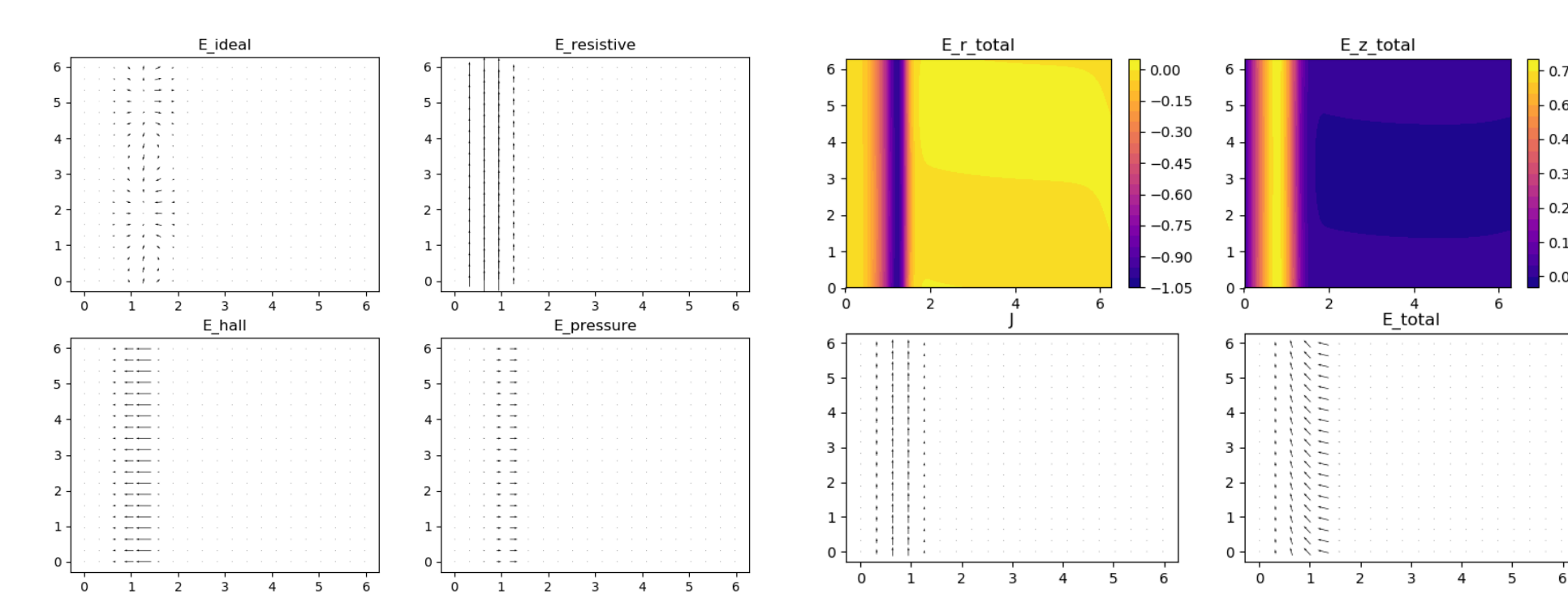


Figure 10. Contours and quiver plots of  $\mathbf{J}$  and  $\mathbf{E}$ .

**Nonlinear Simulations** We solved the ideal MHD equations directly in 2D using central-differencing on a 192x192 grid. To seed the simulation, the equilibrium pressure and density profiles were multiplied by  $1 - 0.01 \cos kz$ . We set periodic boundary conditions in z and we take  $k=1$ . The solution is numerically stable up until shock formation after about  $t=7$ .

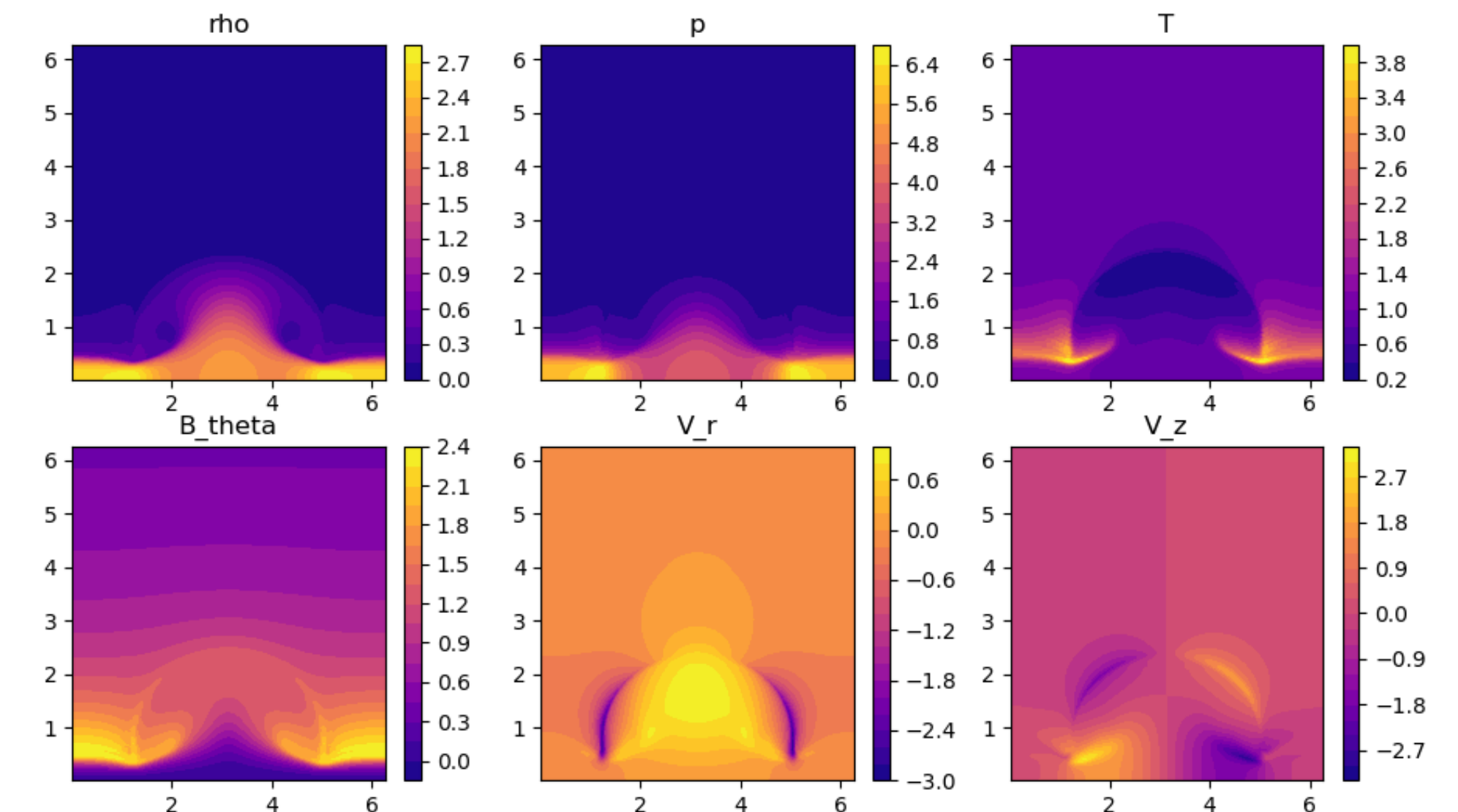


Figure 11. Ideal MHD simulation at  $t=7$ . An artificial viscosity of the form  $\nu \nabla^2 \mathbf{V}$  was added to the momentum equation (neglecting viscous dissipation in the energy equation), with  $v=0.01$ .

The failure of central-differencing to capture shocks motivates the use of WENO (weighted essentially non-oscillatory) schemes [6] to better handle the spatial discretization. A 5th order WENO finite-difference scheme with a Lax-Friedrichs flux splitting was implemented for solving the 1D Burgers' equation and Euler equations as test cases. A 3rd order Runge-Kutta method was used for the time discretization. The WENO scheme is able to handle shock capturing well with some numerical diffusion at shock fronts. For the Euler equations, a component-wise reconstruction was done; we observed numerical oscillations near some shock fronts when solving the Sod, Lax, and Shu-Osher test problems.

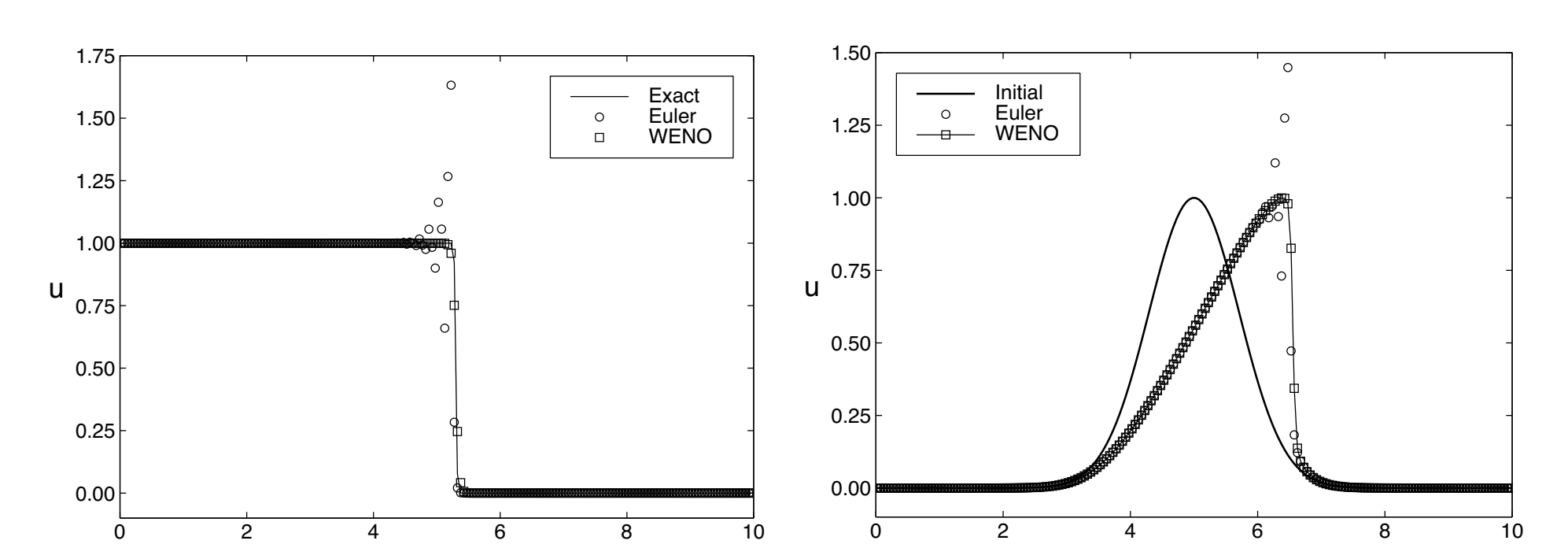


Figure 12. Burgers' equation with 200 grid points. Left: traveling wave solution at  $t=0.6$  as compared to the exact solution, setting  $v=0.005$ . Right: time-evolved Gaussian at  $t=1.4$ , setting  $v=0$ .

**Future Directions** The Hall term presents a promising avenue in investigating charged particle acceleration. A linear stability analysis has shown increased growth rates and a breaking of the mirror symmetry across z. Our linear solver is also easily generalizable to include effects of electron inertia, the displacement current, and a more complex equation of state.

Work is being done on applying WENO to the 2D ideal/resistive MHD equations in the r-z plane using characteristic-wise reconstruction, which is more robust compared to component-wise reconstruction. Comparisons made with Athena++ will be made in both slab and cylindrical geometries. To resolve the pinch at later times, a nonuniform grid will also have to be considered, with many more grid points near  $r=0$ .

## References

- [1] A. S. Richardson et al., in *APS Division of Plasma Physics Meeting* (2016)
- [2] M. G. Haines, *Plasma Phys. Control. Fusion* **53**:093001 (2011)
- [3] D. L. Book, E. Ott, and M. Lampe, *Phys. Fluids* **19**:1982-1986 (1976)
- [4] S. Chandrasekhar, *Hydrodynamic and Hydromagnetic Stability*, Oxford: Clarendon Press (1961)
- [5] D. D. Ryutov, M. S. Derzon, and M. K. Matzen, *Rev. Mod. Phys* **72**:167-223 (2000)
- [6] G. Jiang and C.-W. Shu, *J. Comput. Phys* **126**:202-228 (1996)
- [7] G. Jiang and C. Wu, *J. Comput. Phys* **150**:561-594 (1999)